VOL. 11, NO. 5, MARCH 2016 ISSN 1819-6608
ARPN Journal of Engineering and Applied Sciences

www.arpnjournals.com

NUMERICAL STUDY ON THE DISTANCE-DEPENDENCE OF OPTIMAL LOOP SIZE-RATIOS FOR INDUCTIVE COUPLING LINKS

Akaa Agbaeze Eteng, Sharul Kamal Abdul Rahim and Chee Yen Leow
Wireless Communication Centre, Universiti Teknologi Malaysia, Skudai, Johor, Malaysia
E-Mail: sharulkamal@fke.utm.my

ABSTRACT

Loop sizes are critical to the transfer efficiencies of inductive coupling implementations of wireless power transfer. This contribution is a numerical study of the impact of separation distances between coupled loops on the optimal size-ratios of square loops. Closed-form analytic expressions are developed as a basis for a parametric analysis of link performance parameters. The study leads to the development of a simple design equation to enable the direct determination of optimal relative sizing of coupled loops at required separation distances. The performance enhancement arising from the use of analytically-derived loop-size relationships is confirmed through full-wave electromagnetic simulations.

Keywords: loop size-ratios, numerical, distance-dependence, inductive coupling.

INTRODUCTION

Inductive coupling links for wireless power transfer have, in recent times, received considerable research interest. There are numerous applications for the technology, ranging from power delivery to implanted medical devices, to wireless battery charging implementations for electric vehicles and portable electronic devices [1-4].

Quite often, analyses of inductive coupling links are based on the use of equal-sized loop pairs [5-7]. Although an earlier study suggests that equal-sized loops outperform size-mismatched loop pairs in an un-tuned link scenario [8], there are indications of the non-optimality of equal-sized loops in tuned inductive coupling links [9]. Some algorithms have been developed to design inductive links on the basis of differentials in loop sizes and turn ratios [10-11]. However, not much insight has been provided on the relationship between the optimality of loop size-ratios and the separation distances between them.

Consequently, this paper presents an analysis of the relationship between optimal loop sizing and the separation distance between coupled loop pairs, with a focus on square loops. Numerical studies are employed to reveal relationships between relative loop sizes, and link performance parameters at varying separation distances between the loops. The results show that, for the range of distances considered, equal square loop sizes are generally sub-optimal. Larger separation distances between coupled square loops are shown to require an increase in the size of the transmit loop to maintain optimal performance. However, as the separation distance between coupled loops is reduced, the optimal loop configuration tends towards equal-sized loops. Finally, the paper proposes a design formula to compute the optimal square loop size ratio within the given range of loop separation distances.

MODELLING THE INDUCTIVE LINK

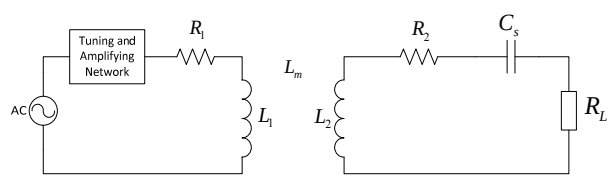

Figure-1. Simple circuit model of inductive coupling link.

Figure-1 is a simple electrical model of a pair of square loops coupled in an inductive coupling link. The capacitance C_s tunes the receive loop to the required operating frequency ω. L_m is the mutual inductance between the coupled loops, while R_L is a resistive model of the electrical load. For ease of modelling, the parasitic capacitances in the loops have been ignored.

The receiver circuit is sensed at the transmitter circuit as a reflected impedance, given by:

$$Z_R = \frac{V_R}{I_1}, \tag{1}$$

where V_R is a reflected voltage. The reflected impedance can be expanded to

$$Z_R = \frac{\omega^4 C_s L_m^2 (R_L + R_2)}{(\omega^2 C_s L_2 - 1)^2 + \omega^2 C_s^2 (R_L + R_2)^2} - j\frac{\omega^3 C_s L_m^2 (\omega^2 C_s L_2 - 1)}{(\omega^2 C_s L_2 - 1)^2 + \omega^2 C_s^2 (R_L + R_2)^2}. \tag{2}$$

If the frequency of operation is defined as

$$\omega = \frac{1}{\sqrt{C_s L_2}}, \tag{3}$$

then (2) reduces to

$$Z_R = \frac{\omega^2 L_m^{\ 2}}{R_2 + R_L}. \quad (4)$$

The efficiency at the transmit loop is therefore

$$\eta_{tx} = \frac{Z_R}{R_1 + Z_R}. \quad (5)$$

Meanwhile, the efficiency of power transfer to the load at the receive loop is given by

$$\eta_{rx} = \frac{R_L}{R_2 + R_L}, \quad (6)$$

so that the transfer efficiency from the transmit loop to the load is

$$\eta_T = \frac{Z_R}{R_1 + Z_R} \cdot \frac{R_L}{R_2 + R_L}. \quad (7)$$

This transfer efficiency is maximized when the connected load is optimal, which is defined in [12] as

$$R_L = \sqrt{\frac{R_2}{R_1}\omega^2 L_m^{\ 2} + R_2^{\ 2}}. \quad (8)$$

Consequently, by substituting (4) and (8) in (7), and applying the relations $Q = \sqrt{Q_1 Q_2}$, $Q_{1,2} = \frac{\omega L_{1,2}}{R_{1,2}}$, $k = \frac{L_m}{\sqrt{L_1 L_2}}$, the maximized transfer efficiency becomes[12]

$$\eta_T = \left(\frac{kQ}{1 + \sqrt{1 + (kQ)^2}} \right)^2. \quad (9)$$

The transfer efficiency, as defined in (9), is completely determined by a figure-of-merit (FoM) kQ – the product of the mean of loop Q-factors, and the coupling coefficient of the inductive coupling link. Ultimately, this FoM is a function of link inductances $L_{1,2,m}$ and resistances $R_{1,2}$.

The inductance of each loop can be related to the physical loop geometry. The inductance of a square spiral loop can be determined by[13]

$$L_{1,2} = 0.635 \mu N^2 d_{avg} \left[\ln\left(\frac{2.07}{\vartheta} \right) + 0.18\vartheta + 0.13\vartheta^2 \right]. \quad (10)$$

μ is the conductor permeability, while the conductor trace fill-factor is given as

$$\vartheta = \frac{d_o - d_i}{d_o + d_i} \quad (11)$$

d_o and d_i refer to the side-lengths of the outermost and innermost loop turns. d_{avg} is the average side length, given by

$$d_{avg} = \frac{d_o + d_i}{2}. \quad (12)$$

Also, the mutual inductance between a coupled pair of square spiral loops is given in [11] as

$$L_m = 1.1 \sum_{i=1}^{N_1} \sum_{j=1}^{N_2} \left(\mu \sqrt{\frac{d_{i_1} d_{j_2}}{4}} \left[\left(\frac{2}{\kappa} - \kappa \right) K(\kappa) - \frac{2}{\kappa} E(\kappa) \right] \right), \quad (13)$$

where d_{i_1} and d_{j_2} are side-lengths of the *i*-th and *j*-th turns of first and second *N*-turn square spiral loops. $K(\kappa)$ and $E(\kappa)$ are the complete first and second kind elliptic integrals, with κ defined as

$$\kappa = \frac{2\sqrt{d_{i_1} d_{j_2}}}{\sqrt{(d_{i_1} + d_{j_2})^2 + z^2}} \qquad i_1, j_2 = 1, ..., N_{1,2}. \quad (14)$$

z refers to the axial distance between the coupled spiral loops.

Taking a cue from [14], the side-length of the outermost loop turn d_o can be related to an optimum axial distance from the loop at which the excited magnetic field is maximum. For a square loop, this distance is determined in [15] as

$$z_0 = \frac{d_0}{2.544} \quad (15)$$

The d.c. resistance of each square loop can be computed from

$$R_{dc} = \frac{4 d_0}{\sigma t w}, \quad (16)$$

where w is the width of the loop turn, t is the thickness of the turn, and σ is the conductivity of the loop conductor. Hence, the a.c. resistance of each loop can be calculated as[11]

$$R_{1,2} = \frac{R_{dc} t}{\sqrt{\frac{2}{\sigma \mu \omega}} \left(1 - e^{-t / \sqrt{\frac{2}{\sigma \mu \omega}}} \right)}, \quad (17)$$

where $\omega = 2\pi f$.

For a coupled pair of loops, (10) – (14), (16) and (17) provide the basis for the determination of the link FoM. The Q-factor of each loop can be calculated by substituting (10) and (17) into (18), which is given below:

$$Q_{1,2} = \frac{\omega L_{1,2}}{R_{1,2}}, \quad (18)$$

VOL. 11, NO. 5, MARCH 2016 ISSN 1819-6608
ARPN Journal of Engineering and Applied Sciences

www.arpnjournals.com

Similarly, the coupling coefficient of the link can be determined by substituting (10) and (13) into (19), which is given below.

$$k = \frac{L_m}{\sqrt{L_1 L_2}}. \tag{19}$$

RESULTS AND DISCUSSION

The developed analytical models were applied in MATLAB numerical simulations to study the variation of link parameters with changes in the axial distance between a pair of coupled square spiral loops. The loop parameters are listed in Table-1.

Table-1. Parameters for numerical simulations.

Parameter	Value
Receive Loop side-length d_0(Rx)	25.44 mm
Reference separation distance z_0	10 mm
Frequency f	13.56 MHz
Turn-width w	1 mm
Turn-thickness t	35 µm
Conductor conductivity σ	5.8 x 10^8 S/m
Conductor absolute permeability μ	1.2566 x 10^{-6}

Figure-2 shows the variation of coupling coefficient with distance for a pair of single-turn square spiral loops. The ratio of side-length of the transmit loop to side-length of the receive loop is increased from 0.5/1 to 4/1. The plot shows that when the separation between the loops is almost 0, the strongest coupling is achieved with practically equal-sized loops. However, as the separation distance tends towards z_0 and beyond, the coupling drops drastically, and the peak coupling is achieved with slightly increasing sizes of the transmit loop relative to the receive loop.

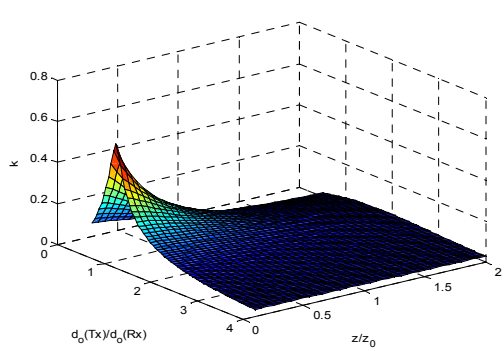

Figure-2. *k* with distance and side-length ratio (1 turn).

Figure-3 examines the same relationship between side-length ratios, separation distance and coupling coefficient for a pair of 4-turn square spiral loops. The results show the same trend in coupling levels with distance, although the peak coupling levels are higher than obtained using paired single-turn loops.

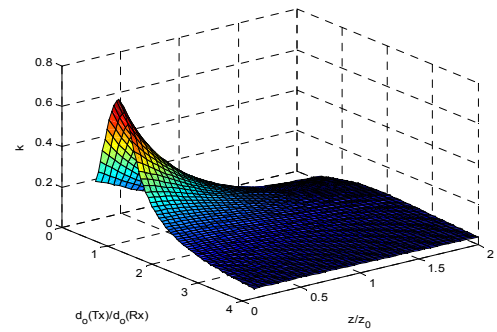

Figure-3. *k* with distance and side-length ratio (4 turns).

Figure-4 and Figure-5 demonstrate the effect of changes in loop size ratio and separation distance on the mean of Q-factors for single-turn and 4-turn loops.

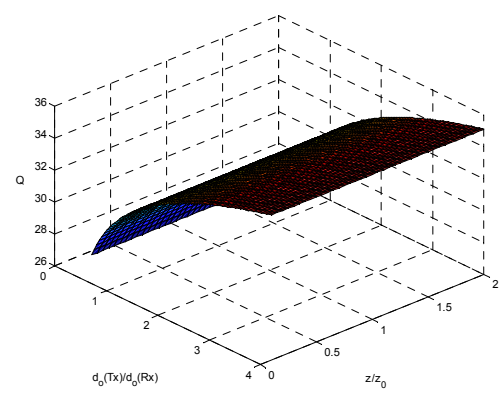

Figure-4. Q with distance and side-length ratio (1 turn).

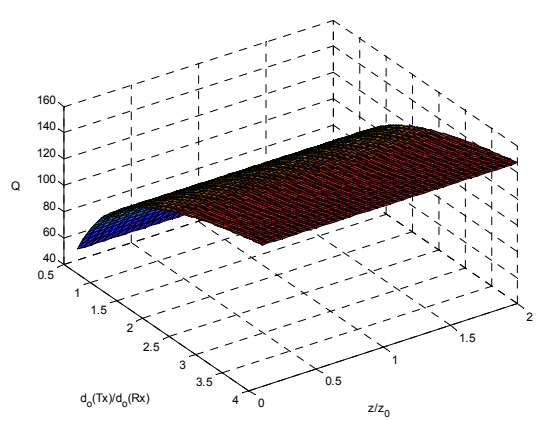

Figure-5. Q with distance and side-length ratio (4 turns).

Expectedly, the separation distance has no effect on the Q-factor level. However, the mean Q-factor level increases with increasing size of the transmit loop. The increase in mean Q-factor is initially rapid, but slows

down as the side-length of the transmit loop approaches 4 times the side-length of the receive loop.

Figures-2-5 reveal trends in parameter values with changes in separation distance and loop side-length ratios that are largely independent of the number of turns in a loop. Figure-6, therefore, examines the effects of range and length ratios on the FoM of a link comprising of single-turn square loops, which could be generalized to multi-turn configurations.

It can be observed from Figure-6 that the side-length ratio that yields the highest FoM level rises with an increase in the separation distance between loops.

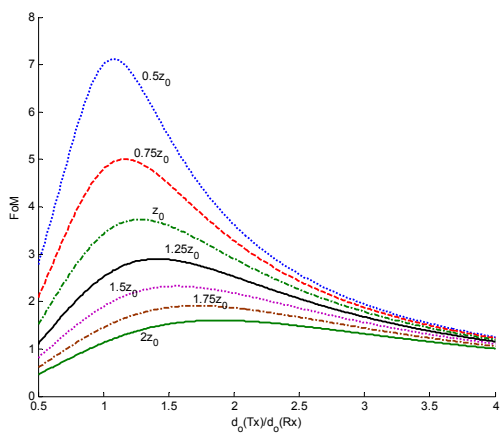

Figure-6. Side-length ratio vs FoM for different distances.

It is also interesting to note that, for a loop separation distance in the range of $0.5z_0 \le z \le 2z_0$, the coupling of equal-sized loops with the same number of turns provides sub-optimal link performance. Indeed, the result suggests that, within the stated distance interval, optimal link performance requires the use of larger transmit loops relative to receive loops. Also, the optimal relative size of the transmit loop increases as the separation distance from the receive loop is increased.

Figure-7 shows the fitting of a fifth-degree polynomial to the data points representing the points of optimal FoM level for the simulated data in Figure- 6, namely:

$$y = -0.11x^5 + 0.69x^4 - 1.75x^3 + 2.29x^2 - 1.10x + 1.21, \quad (20)$$

where $y = d_0(\text{Tx})/d_0(\text{Rx})$, and $x = z/z_0$. This expression calculates the appropriate transmit-to-receive loop side-length ratio to achieve optimum FoM levels within the range interval $0.5z_0 \le z \le 2z_0$.

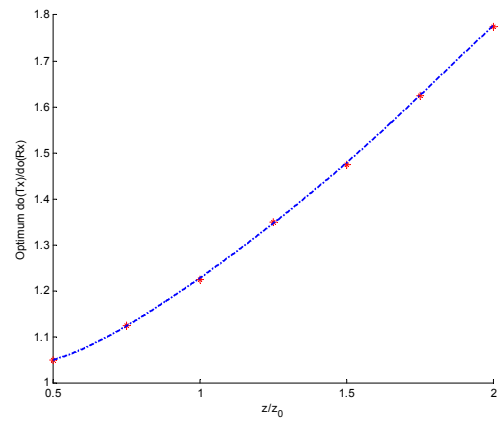

Figure-7. Polynomial fitting for optimum side-length ratio for $0.5z_0 \le z \le 2z_0$.

To confirm the analytically derived distance-dependence of optimal loop size-ratios, full-wave electromagnetic (EM) simulations of two coupled inductive coupling links, using single-turn square loops, were performed in CST Microwave Studio. The EM simulations were used to extract inductance, resistance and mutual inductance values of the modelled loops at 13.56 MHz, which were then employed to compute link FoMs and transfer efficiencies. The results are tabulated in Table-2.

Table-2. EM Simulation results.

Parameter	EM Simulation Results	
	Equal sized	Unequal sized
Side-length ratio $d_0(\text{Tx})/d_0(\text{Rx})$	1/1	1.69/1
FoM (10 mm) FoM (20 mm)	12.21 4.68	11.39 6.10
η_T (10 mm)	84.91 %	83.91 %
η_T (20 mm)	65.42 %	72.15 %

The first link comprised of the conventionally employed equal-sized loops, where the side-lengths were determined using (15) for a range z_0 = 10 mm. The second link comprised of a similar-sized receive loop, while the side-length of the transmit loop was computed from (20) for $z = 2z_0$. The FoM and transfer efficiency values for both links were obtained for $z = z_0$ and $z = 2z_0$. All loops were modelled using FR4 photoresist boards, with dielectric constant of 4.7 and loss tangent of 0.019.

The tabulated results show that the first link with equal-sized loops provides a higher transfer efficiency at z =10 mm than the link with unequal sized loops. This is in keeping with the analytical results in Figure-7, where, for $z = z_0$, a 1/1 ratio of side-lengths of transmit and

receive loops is closer to optimum than the 1.69/1 ratio provided in the second link. However, the second link has a higher transfer efficiency than the conventional arrangement at z =20 mm. This is because the 1.69/1 side-length ratio used in the second link is optimal for $z = 2z_0$, as derived from (20).

CONCLUSIONS

This paper has studied the dependence of optimal size-ratios of a pair of coupled loops in an inductive coupling link on the separation distance between the loops. The analysis presented shows that equal-sized loop pairs provide sub-optimum levels of link transfer efficiency as the distance between a coupled pair of loops, with similar number of turns, is increased. In addition, the paper has provided a simple design formula to enable the determination of an optimal ratio of side-lengths for a coupled pair of square loops with same number of turns, within a range of separation distances.

ACKNOWLEDGEMENTS

This research is supported by the Ministry of Education Malaysia, and Universiti Teknologi Malaysia, under grant numbers 4F617, 4F290, 4F261 and 05H39. The grants are managed by the Research Management Center, Universiti Teknologi Malaysia.

REFERENCES

[1] Ramrakhyani A. K. and Lazzi, G. 2013. On the design of efficient multi-loop telemetry system for biomedical implants. IEEE Transactions on Biomedical Circuits and Systems. 7(1): 11–23.

[2] Wang G., Wang P., Tang Y. and Wentai L. 2012. Analysis of dual band power and data telemetry for biomedical implants. IEEE Transactions on Biomedical Circuits and Systems. 6(3): 208–15.

[3] Eberle W. and Musavi F. 2014. Overview of wireless power transfer technologies for electric vehicle battery charging. IET Power Electronics. 7(1): 60–66.

[4] Hui, S. Y. 2013. Planar Wireless Charging Technology for Portable Electronic Products and Qi. Proceedings of IEEE. 101(6): 1290–1301.

[5] Zhang Y. and Zhao Z. 2014. Frequency Splitting Analysis of Two-Loop Resonant Wireless Power Transfer. IEEE Antennas and Wireless Propagation Letters 13: 400–402.

[6] Zhou H., Zhu B., Hu W., Liu Z. and Gao X. 2014. Modelling and Practical Implementation of 2-Coil Wireless Power Transfer Systems. Journal of Electrical and Computer Engineering. 2014: 1–8.

[7] Inagaki, N. 2014. Theory of Image Impedance Matching for Inductively Coupled Power Transfer Systems. IEEE Transactions on Microwave Theory and Techniques. 62(4): 901–908.

[8] Eteng A., Rahim S. K. A. and Leow C. Y. 2014. Effects of Size Mismatch in Dual-function Near-Field Antennas. In: IEEE Asia Pacific Conference on Wireless and Mobile. pp. 260–263.

[9] Bosshard R., Muhlethaler J., Kolar J. W. and Stevanovic I. 2013. Optimized magnetic design for inductive power transfer loops. In: Applied Power Electronics Conference and Exposition. pp. 1812–1819.

[10] Waters B. H., Mahoney B. J., Lee G. and Smith J. R. Optimal loop size ratios for wireless power transfer applications. 2014. In: 2014 IEEE International Symposium on Circuits and Systems 1(1): 2045–2048.

[11] Jow U. and Ghovanloo M. 2007. Design and optimization of printed spiral loops for efficient transcutaneous inductive power transmission. IEEE Transactions on Biomedical Circuits and Systems. 1(3):193–202.

[12] Strömmer E., Jurvansuu, M., Tuikka, T., Ylisaukko-Oja A., Rapakko H. and Vesterinen J. 2012. NFC-enabled wireless charging. In: Proceedings - 4th International Workshop on Near Field Communication. pp. 36–41.

[13] Mohan S. S., del Mar Hershenson, M., Boyd S. P. and Lee T. H. 1999. Simple accurate expressions for planar spiral inductances," IEEE J. Solid-State Circuits, vol. 34, no. 10, pp. 1419–1424.

[14] Aerts W., De Mulder E., Preneel B., Vandenbosch G. A. E. and Verbauwhede I. Dependence of RFID Reader Antenna Design on Read Out Distance. IEEE Transactions on Antennas and Propagation. 56(12): 3829–3837.

[15] Eteng A., Abdul Rahim S. and Leow C. 2015. Geometrical Enhancement of Planar Loop Antennas for Inductive Near-Field Data Links. IEEE Antennas and Wireless Propagation Letters. (in press).

[16] Sample A. P., Meyer D. A. and Smith J. R. 2011. Analysis, Experimental Results, and Range Adaptation of Magnetically Coupled Resonators for Wireless Power Transfer. IEEE Transactions on Industrial Electronics. 58(2): 544–554.